ResearchGate

See discussions, stats, and author profiles for this publication at: https://www.researchgate.net/publication/335002060

Ionospheric Response to the Space Weather Events of 4–10 September 2017: First Chilean Observations

Article *in* The Open Atmospheric Science Journal · June 2019

CITATIONS
3

READS
314

7 authors, including:



Manuel Alejandro Bravo Sepulveda
Universidad Adventista de Chile
23 PUBLICATIONS **97** CITATIONS
SEE PROFILE



Carlos Ulises Villalobos
Universidad Adventista de Chile
7 PUBLICATIONS **38** CITATIONS
SEE PROFILE



Rodrigo Leiva
Universidad Adventista de Chile
5 PUBLICATIONS **23** CITATIONS
SEE PROFILE



Luis Tamblay
University of La Serena
5 PUBLICATIONS **22** CITATIONS
SEE PROFILE

All content following this page was uploaded by Alberto J. Foppiano on 06 August 2019.

The user has requested enhancement of the downloaded file.



The Open Atmospheric Science Journal

Content list available at: https://openatmosphericsciencejournal.com

RESEARCH ARTICLE

Ionospheric Response to the Space Weather Events of 4-10 September 2017: First Chilean Observations

Manuel Bravo[1,*], Carlos Villalobos[2], Rodrigo Leiva[3], Luis Tamblay[4], Pedro Vega-Jorquera[4], Elías Ovalle[5] and Alberto Foppiano[5]

[1]*Departamento de Geofísica, Universidad de Concepción, Chile*
[2]*Facultad de Educación, Universidad Adventista de Chile, Chillán, Chile*
[3]*Facultad de Ingeniería y Negocios, Universidad Adventista de Chile, Chillán, Chile*
[4]*Departamento de Física y Astronomía, Universidad de La Serena, La Serena, Chile*
[5]*Departamento de Geofísica, Universidad de Concepción, Concepción, Chile*

Abstract:

Objective:

The diurnal variations of several ionospheric characteristics during the Space Weather Events of 4-10 September 2017, for Chilean latitudes, will be reported.

Materials and Methods:

Observations were made using a recently installed ionosonde at the Universidad de La Serena field station (29°52'S; 71°15'W). Also, reported is the total electron content determined using the upgraded Chilean network of dual-frequency Global Navigation Satellite Systems (GNSS) receivers.

Results:

Sudden ionospheric disturbances are described in terms of the minimum reflection frequency determined from ionosonde records. An attempt to derive the extent of the effect on high frequency propagation paths in the region is made using simultaneous ionosonde observations at other locations.

The geomagnetic storm ionospheric effects are discussed in detail using the observed diurnal variation of maximum electron concentration (NmF2), virtual height of the F-region (h'F/F2) and Total Electron Content (TEC). These are complemented with the time-latitude variation of TEC for the 70°W meridian.

Conclusion:

It is found that large increases of NmF2, h'F/F2 and TEC observed during 8 September 2017 storm are well described in terms of the evolution of the Equatorial Ionospheric Anomaly (EIA) over the same time interval. Known physical mechanisms are suggested to explain most of the observations.

Keywords: Ionospheric disturbance, September 2017 space weather event, Mid-latitude , equatorial observations, Ionospheric response, GNSS.

Article History	Received: January 16, 2019	Revised: April 24, 2019	Accepted: May 260, 2019

1. INTRODUCTION

It is well known that geomagnetic storms generate ionospheric disturbances. These disturbances have been reported around the world [1 , 2]. Initially, ionospheric disturbances were detected in communications using radio wave propagation, then, they were measured as disturbances on vertical incidence radar (ionosonde) observations. Today, it is possible to detect ionospheric disturbances with satellites, rockets, incoherent scatter radars, coherent radars, all-sky imagers, among other instrumentation. Using both space- and

* Address correspondence to this author at Departamento de Física,Universidad de Concepción, Casilla 160-C Concepción, Chile; Tel: +56 41 2203083; E-mail: mbravo@dgeo.udec.cl

ground-based concurrent observations, it is possible to obtain good temporal and spatial resolutions of the observations.

Reports of regional studies of the effects of geomagnetic storms have been made (*e.g.* Italy, North Africa and Brazil), as multi instrument ionospheric observations have become available [3 - 8]. One regional study relates the increases of maximum electron concentration (NmF2), Total Electron Content (TEC) and airglow intensity for several hours during a geomagnetic storm (13-15 November 2012) associated with northward evolution of the Equatorial Ionospheric Anomaly (EIA) in the northern hemisphere [3]. Other reports [4] on the generation of traveling ionospheric/thermospheric perturbations by a geomagnetic storm (27-28 February 2014). They found anti-correlation between observed NmF2 and the height of the maximum of maximum electron concentration (hmF2).

Specifically, for the South American sector, geomagnetic storms with associated ionospheric disturbances have been reported in studies [5 - 9], among others, using observations made by some instruments deployed over Brazil and Perú. These are considered particularly valuable because it has long been recognized that the structures of the thermosphere and ionosphere may be unique along the longitude sector containing South America and the Antarctic Peninsula. For these locations, solar associated effects (which are better represented in geographic latitude) are probably well separated from geomagnetic effects (which depend on geomagnetic latitude) [10]. In particular, modelling using the Coupled Thermosphere-Ionosphere-Plasmasphere model [11] has shown that the relation between thermospheric circulation, vertical motions, and composition changes has specific characteristics in this longitude sector [12 - 14], a sector identified by leading ionospheric physicist [15] as “far-from-pole” (magnetic pole). Along these longitudes, the equatorial boundaries of the auroral zones, where energy is received in the thermosphere from electric fields and particle precipitation generated by magnetospheric processes, are farther away from the equator than elsewhere in the southern hemisphere. Furthermore, due to the offsets of the magnetic poles the geographic latitudes of these boundaries change with longitude by about 15° in the southern hemisphere as compared with only 8° in the northern hemisphere [12]. Moreover, eastern South America and the Antarctic Peninsula are on the westward slope of the South Atlantic Geomagnetic Anomaly, making the longitude sector unique globally. The effects of geomagnetic storms on the ionosphere in this sector also seem to be different from those at other locations [16 - 18].

The purpose of the present paper is to report on the ionospheric response observed in Chile to the Space Weather Events of 4-10 September 2017. In particular, this paper describes the ionospheric effects of multiple solar X-ray flares (intensity and evolution) and of the ensuing geomagnetic storms for low and middle latitudes within a rather special longitude sector. Moreover, this paper examines the association between the effects on different ionospheric characteristics on the grounds of known physical mechanisms.

This paper is unique as it presents the first ever observations of ionospheric characteristics made by an ionosonde at La Serena. Moreover, the TEC determinations reported here are from the densest network of Global Navigation Satellite Systems (GNSS) receivers available in Chile. Only a subset of this network was used in a previous study [19].

2. MATERIALS AND METHODS

After the great Chilean earthquake of 27 February 2010, some significant changes in ionospheric observations have taken place within Chile.

First, the long-time operated Concepción Station (36°47’S; 73°02’W) was relocated at the Universidad Adventista de Chile, Chillán (36°38’S; 72°00’W). This is 91.1 km along with the 80°09’ East of North azimuth. A Canadian Advanced Digital Ionosonde (CADI) and an Ionospheric Prediction Service (IPS-42) ionosonde were deployed [20]. The first CADI ionogram was taken on 9 August 2012 at 16:18 LT (75°W). Later on, a new ionospheric station was established at a field station of Universidad de La Serena (LS, 29°52'S; 71°15’W), La Serena, and the IPS-42 was deployed there. Ionospheric soundings were started on 24 August 2017. A short report on these soundings was given in a conference presentation [21].

A second development on ionospheric observations arises from the tenfold increase in the Chilean network of dual-frequency GNSS receivers set up by the Centro Sismológico Nacional (National Seismological Centre, CSN in Spanish). These allow TEC determinations over most of the continental Chile. The locations of the receivers are indicated in Fig. (**1**) together with those of the two ionosondes.

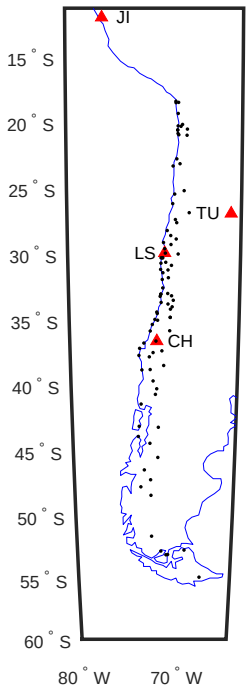


Fig. (1). Locations of (triangles) ionosondes and (dots) GPS receivers. Chillán (CH, 36°38’S; 72°00’W), Jicamarca (JI, 11°57’S; 78°52’W), La Serena (LS, 29°52'S; 71°15’W) and Tucumán (TU, 26°50’; 65°14’W).

2.1. Ionospheric Characteristics From Ionosonde

Digital ionograms obtained at 15 min intervals from 26 August to 24 September 2017 with the IPS-42 ionosonde at LS were manually scaled using the DIGION programme [22]. Seven ionospheric characteristics were determined, *i.e.* fmin, foE, ftEs, foF2, h'E, h'F/F2 and M3000F2 (see a brief meaning description in List of Abbreviations). NmF2 was then calculated using the standard formula as: $NmF2=1.24\cdot10^{10}(foF2)^2$ [23]. foF2 is in MHz and NmF2 in m^{-3}. Reference values for each ionospheric characteristic were calculated as the median values at 15 min intervals from 17 days selected within the observed interval, since these days are considered geomagnetically unperturbed. Thirteen days fulfill the Ap ≤ 10 and Dst ≥ -25 criteria. However, there are four days that although qualify for the Dst condition, do not qualify for the Ap condition. These days are included so as to minimize ionospheric observations gaps, and because no significant geomagnetic perturbations were observed during them. Moreover, leaving out those four days does not alter the shape of the diurnal variations. A reference lower boundary, as the median minus the interquartile range, and a reference upper boundary, as the median plus the range, were also computed. A 9-point running mean was applied to all three reference series of values. The variability of a given ionospheric characteristic is specified as the difference between the reference upper boundary and reference lower boundary. Diurnal variations of global geomagnetic indices and LS ionospheric character- istics NmF2, h'F/F2 and fmin, for 3 September 2017 are given in Fig. (**2**) . They are shown because 3rd September 2017 is one of the few days for which observations are available all day long. Unfortunately, no ionosonde observations were made during the studied time interval at the Chillán ionosonde due to the CADI failure. Geophysical information on ionosondes/digisonde used is presented in Table **1**.

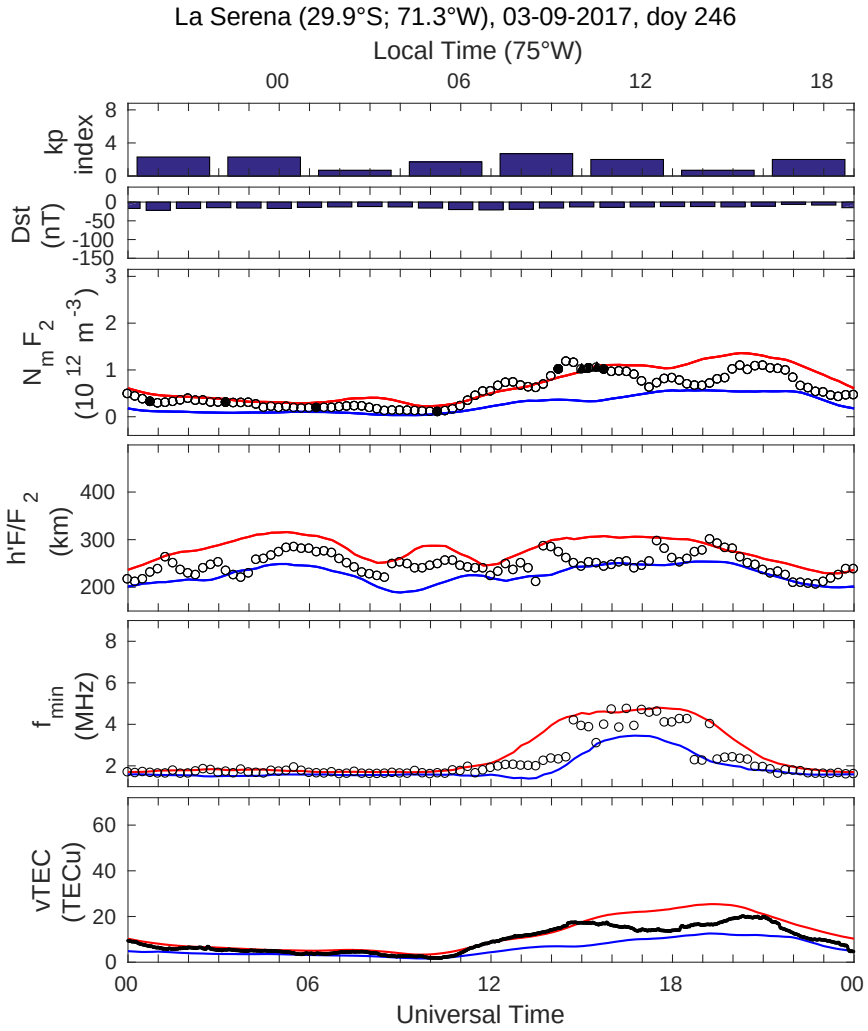


Fig. (2). Diurnal variations of global geomagnetic indices and La Serena (29°52'S; 71°15'W) ionospheric characteristics and vTEC for 3 September 2017. (a) kp. (b) Dst. (c) NmF2. (d) h'F/F2. (e) fmin. (f) vTEC. Open circles, black filled circles and a black line are observed values; black filled circles are for those values scaled as "doubtful" according to international accepted rules [34]. Red lines are for smoothed median values plus interquartile range and blue lines are for the median minus interquartile range for 17 quiet days.

Table 1. Geographical and geophysical information of the ionosonde/digisonde stations mentioned in this work.

Station	Geographical Latitude	Geographical Longitude	Geomagnetic Latitude	Magnetic Declination	DIP Angle
La Serena (LS)	-29.9°	288.7°	-16.5°	0.7°	-30.7°
Chillán (CH)	-36.6°	288.0°	-21.2°	6.8°	-37.8°
Tucumán (TU)	-26.9°	294.6°	-14.9°	-5.5°	-28.1°
Jicamarca (JI)	-12.0°	283.2°	0.2°	-1.6°	-0.5°

2.2. Total Electron Content From Gps Observations

TEC was calculated with a 1 min time resolution using the program in a study [24] from Receiver Independent Exchange Format (RINEX) files for 91 stations that were made available by the Centro Sismológico Nacional (http:// www.sismologia.cl), Universidad de Chile, from September 2016 onwards. For only 6 of these stations RINEX files are available at the International GNSS Service (IGS). This software calculates the slant TEC (sTEC) from pseudo-ranges measurements of each GNSS receiver (note that data from RINEX files are available at 30 seconds intervals). The clock errors and tropospheric effects are eliminated using the phase and code values for the transmitted L1 and L2 GPS frequencies. Differential satellite biases and receiver bias are included to obtain absolute values of sTEC. Finally, the satellite elevation and azimuth angles are used in the calculation of vertical TEC (vTEC) from sTEC. We have used vTEC values corresponding to satellite elevation angles ≥30° in order to minimize possible errors.

Mean vTEC is computed along three longitude bands 5° wide, using values from all GPS receivers within two-degree latitude intervals. These mean values are assigned to longitudes 75°, 70° and 65°W. Reference median, lower boundary and upper boundary values were computed in the same way as those selected for the ionosonde observed ionospheric characteristics. Fig. (**2**) shows the sample diurnal variation of vTEC for 3 September 2017 corresponding to LS computed as the mean assigned to the 28°-30°S latitude range and the 70°W longitude. Reference lower and upper boundary are also shown.

3. RESULTS

3.1. Sudden Ionospheric Disturbances (SIDs)

A detailed description of the evolution of various characteristics of solar and geomagnetic activities during the Space Weather Events of 4-10 September 2017 is given in a study [25]. Just for the purpose at hand it is recalled that on the 26 August-24 September 2017 interval, 19 flares with intensities above M1.1 and 4 above X1.3 were observed. Of all these, clear effects are seen on the LS ionosonde observations during the X9.3 flare of 6 and the X8.2 of 10 September 2017. A specific description of some of these flares is also given in a study [26] (Fig. **6**).

Diurnal variations of global geomagnetic indices, ionospheric characteristics for LS, GOES X-ray flux and vTEC for 6 and 10 September 2017 are shown in Fig. (**3**). Also shown are fmin for Jicamarca (JI, 11°57'S; 78°52'W) and Tucuman (TU, 26°50'; 65°14'W). The X-ray fluxes are those observed by the GOES-15 X-ray Sensor (XRS) instrument's "long" band (0.1- 0.8 nm) available at https://satdat.ngdc.noaa.gov. Although it is not possible to identify the SID starting time at LS on 6 September 2017 Fig. (**3**), left), because there is an ionogram gap, fmin decreases steadily from about 6 MHz at 14:00 UT (09:00 LT) to approximately 4 MHz at 20:00 UT (15:00 LT). At nearly all times fmin is above the reference upper boundary and the linear decrease rate for the 14:00 to 20:00 UT (09:00 to 15:00 LT) is about 0.3 MHz/h. There is also a sudden fmin decrease between 20:00 UT and 21:00 UT (15:00 and 16:00 LT), after which fmin is within the lower and upper reference boundaries. Ionograms from TU, some hundred km North-East of LS show the blackout starts at 11:53 UT (06:53 LT) and ends at 13:03 UT (08:03 LT). For JI, at equatorial latitudes, the blackout starts at 12:00 UT (07:00 LT) and finishes at 13:25 UT (08:25 LT). The corresponding fmin decreases the rate for JI is 0.24 MHz/h, somehow similar to that for LS. No firm statement can be made as to the starting and ending times for the different locations quoted. This lack of certainty is due to the fmin dependency on the ionosonde sensitivity (which depends on the receiver sensitivity and the antennas gain) and on the upper ionosonde frequency limit. Although the upper frequency limit of LS ionosonde is 22.6 MHz as compared with 15 and 16 MHz for TU and JI, the sensitivity of the JI ionosonde is far greater than that for other two ionosondes. This is because it has 42 dB gain just on account of signal processing: phase coded pulse compression (21 dB) and coherent Doppler integration (additional 21 dB).

On 10 September 2017 (Fig. 3, right), the flare onset is at 15:35 UT (10:35 LT), this is 5 min after the last recorded ionogram at LS and 10 min before the following one. However, there is no blackout at 15:45 UT (10:45 LT), fmin is only larger than the reference upper boundary. Blackout is clearly observed from 16:00 to 19:00 UT (11:00 to 14:00 LT). This may be due to the slow increase of the flare radiation intensity since it takes 31 min after for the flare to reach a maximum at 16:06 UT (11:06 LT). The other flares observed between 6 and 10 September 2017 took half of that time. The 10 September 2017 flare intensity decay took 25 min compared to 7 to 19 min for the other flares. The first ionogram showing reflection traces (19:15 UT; 14:15 LT) exhibits a large fmin (6.39 MHz) well above the upper boundary for that hour. The fmin rate of linear decrease in this case is approximately 1.3 MHz/h. Blackout is observed at TU from 15:53 to 16:38 UT (10:53 to 11:38 LT), two hours shorter than at LS. Although blackout starts almost simultaneously at JI (15:58 UT; 10:58 LT), TU and LS, at JI it ends two hours later than at TU. The fmin decrease at JI which is 1.1 MHz/h.

The rates of fmin decrease at LS and JI for the 10 September 2017 X8.2 flare are almost 4 times larger than those

for the 6 September 2017 X9.3 flare. Part of the reason for this difference may be associated with the flare occurrence time: the X9.3 ionospheric effects are mainly morning ones (12:00-20:00 UT; 07:00-15:00 LT) while those for the X8.2 occur in the afternoon (16:00-22:00 UT; 11:00-17:00 LT) when the mean solar zenith angle is smaller. Nevertheless, it is more likely that the major reason relates the particular evolution of the radiation intensity for the two cases.

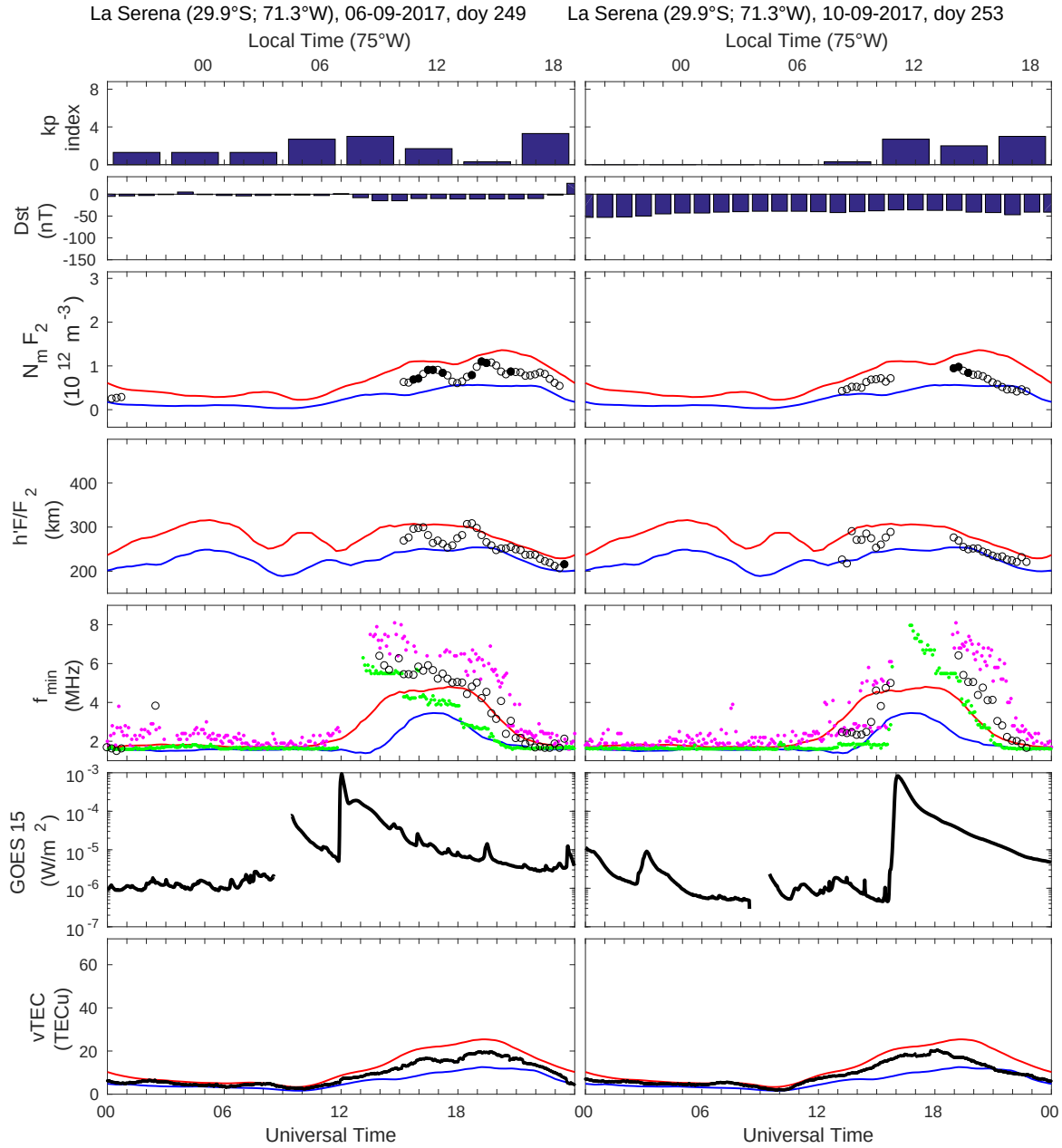


Fig. (3). Diurnal variations of global geomagnetic indices, ionospheric characteristics, GOES X-ray flux and vTEC for 6 (left) and 10 (right) September 2017. (a) kp. (b) Dst. (c) NmF2 and (d) h'F/F2 for La Serena (LS, 29°52'S; 71°15'W). (e) fmin for LS, Jicamarca (JI, 11°57'S; 78°52'W) and Tucuman (TU, 26°50'; 65°14'W). (f) GOES solar X-ray flux and (g) vTEC for LS. Open circles, black filled circles and a black line are for LS; black filled circles are for those values scaled as "doubtful" according to international accepted rules [34]. Red lines are for smoothed median values plus interquartile range and blue lines are for the median minus interquartile range for 17 quiet days. fmin at JI and TU are shown in magenta dots and green dots, respectively.

Since both flares occur near the spring equinox (southern hemisphere), the daytime length (about 12 h) is approximately the same at LS and JI, thus the evolution of the flare radiation is the same at both places. The minimum solar zenith angle is obviously smaller at JI than at LS, but this difference should only affect the intensity and duration of the effect and does not affect its time evolution, provided that other factors are the same (*e.g.* composition).

There are no traces on the LS ionograms for 14:45, 15:00 and 15:15 UT (09:45, 10:00 and 10:15 LT), 7 September 2017, this may be due to instrument failure and not necessarily associated with the 7 September 2017 X1.3 morning flare (14:20, 14:36 and 14:55 UT; 09:20, 09:36 and 09:55 LT, start, maximum and end of flare, respectively). It is true that fmin (Figure not shown) is larger than the reference upper limit from 15:30 through to 16:45 UT (10:30-11:45 LT). However, no typical slowly decreasing is observed. By contrast, ionograms for the whole flare interval observed at TU and JI do show the usual variation of fmin during flares. In particular, fmin at JI changes from 3 to almost 8 MHz within five minutes.

Observations for the 8 September 2017 M2.9, also a morning flare, again show fmin values larger than those expected for unperturbed condition at all LS, TU and JI. This time, the blackout condition at 15:45 UT (10:45 LT) observed over LS is most likely due to increased absorption and not to ionosonde failure as suspected for the 7 September 2017 flare.

The blackouts and large values of fmin already mentioned are consistent with many HF circuit blackouts for equatorial and low latitudes over a range of frequencies. The absorption for oblique incidence HF propagation is always larger than that for corresponding vertical incidence propagation. Thus, at least for blackout conditions (fmin larger than 15 or 16 MHz at TU and JI) HF propagation using frequencies over the whole HF range (3 to 30 MHz) would be impaired. Finally, it is worth noting that TEC observations may not show any effects of the flares already discussed using ionosonde observations. Fig. (**3**) shows the diurnal variations of vTEC for LS determined as indicated before during the 6 and 10 September 2017 flares confirming the absence of the effects. A simple coarse estimation assuming step shape regions indicates that the D- and lower E-region contribution would be about 1% of the F-region. This is for an F-region foF2 = 10 MHz, hmF2 = 250 km, ymF2 (semi-thickness) = 100 km, foD/E = 3.5 MHz, hmE = 100 km and ymD/E = 20 km. However, some effects on TEC seem to be observable using a more refined analysis as reported in studies [27, 28]. In any case, the contribution to vTEC by D- and lower E-region increased ionization due to the flares radiation is indeed small when compared with the contribution of the F-region.

3.2. Ionospheric Storms

3.2.1. Diurnal Variations

Diurnal variations of global geomagnetic indices and ionospheric characteristics NmF2, h'F/F2 and vTEC for LS and TU (assumed to be similar on the grounds of nearness) during the 7 (05:00-24:00 UT), 8 and 9 (00:00-05:00 UT) September 2017 are shown in Fig. (**4**) . Also shown in Fig. (**4**) are NmF2, h'F/F2 and hmF2 for JI.

There are four significant deviations of the ionospheric characteristics from what could be considered as the reference values. The first is an increase of NmF2 at LS, though only suggested by three values (23:45, 00:00, 00:15 UT; 18:45; 19:00; 19:15 LT) in the evening of 7 September 2017. These three values are followed by strong Spread-F up to 06:30 UT (01:30 LT) of 8 September 2017, but this does not preclude another six NmF2 values to be determined around midnight. The ionosphere reflection dispersion in both frequency and height characteristic of the Spread-F condition, sometimes permit height and critical frequency to be determined. The nine values are definitely above the variability range. The NmF2 increase at LS is confirmed over TU. By contrast, a decrease of NmF2 at JI is initially suggested by a few values (near 01:30 UT; 20:30 LT), although some of the following scalings may be less clear due to the prevalent Spread-F. The NmF2 decrease at JI coincides with the vTEC increase observed at LS and TU. The NmF2 increase at LS is clearly related to the large increase of h'F/F2 observed at JI that coincides with the sharp Dst decrease (about -150 nT) corresponding to the storm main phase. Moreover, the JI height increase may be associated with two h'F/F2 increases observed at TU and LS peaking at 02:00 and 03:00 UT (21:00 and 22:00 LT), the latter at 350 km by comparison to the observed LS variability of 220 to 280 km (median plus minus interquartile range). The two peaks take place two and three hours after the h'F/F2 peak observed at JI.

A second deviation from 07:00 UT (02:00 LT) and up to 11:00 UT (06:00 LT) on 8 September 2017 is evident as a significant increase of h'F/F2 and an almost concurrent decrease of NmF2 well observed at TU. The deviation takes place near the end of a first recovery phase of the storm (Dst from about -140 to -60 nT). vTEC at LS is low but within the variability limits. Unfortunately, no ionograms are available at LS due to ionosonde malfunction.

The following significant features are a small h'F/F2 peak observed at LS between 15:30 and 15:45 UT (10:30 and 10:45 LT) on 8 September 2017 (there are two ionograms missing) which occurs just one hour before ensuing large and short lived NmF2 increase. Both h'F/F2 and NmF2 deviations are clearly confirmed at TU. The NmF2 increases are also simultaneous with a corresponding increase of vTEC at LS and TU. No clear corresponding features for these two characteristics are observed at JI. Note there is only a very small increase of NmF2 at JI.

The last deviation from reference values is the very large increase of NmF2 at LS peaking at about 22:30 UT (17:30 LT). It is associated with a small h'F/F2 change just half an hour before. An even larger NmF2 increase is simultaneously observed at TU. The maximum value cannot be determined because the corresponding foF2 is larger than the ionogram upper frequency limit (15 MHz, 2.79×10^{12} m^{-3}). A corresponding very large vTEC simultaneous increase at LS is also evident. The earlier h'F/F2 increase at TU is better identified than that observed at LS. In both cases, h'F/F2 decreases immediately after, reaching a minimum at about 00:00 UT (19:00 LT). No NmF2 increase is observed at JI. As a matter of fact, NmF2 is almost constant over the whole

interval. By contrast to the minimum h'F/F2 at LS and TU, a small simultaneous maximum of h'F/F2 and hmF2 is observed at JI.

3.2.2. Latitudinal Variations

Fig. (**5**) shows the time latitude variation of the observed vTEC along the 70±2.5°W longitude band for 26 August and 8 September 2017, one of the quieter days of the month (q3, Σkp = 6-, Ap = 3; Dst = -4) and the storm day, respectively. The time variations are those as explained in Section 2.2. Although the 28 August 2017 is the quietest day of the month (q1, Σkp = 4+, Ap = 2; Dst =-15), the development of the EIA is not so clearly evident on that day. The EIA is an increase of ionization usually observed at about the geomagnetic equator in the afternoon [29, 30]. Also shown in Fig. (**5**) is an enlargement of the 8 September 2017 variation. In this enlarged figure, there are more gaps or they are larger because the observed mean values correspond to 1° latitude interval instead of 2° latitude.

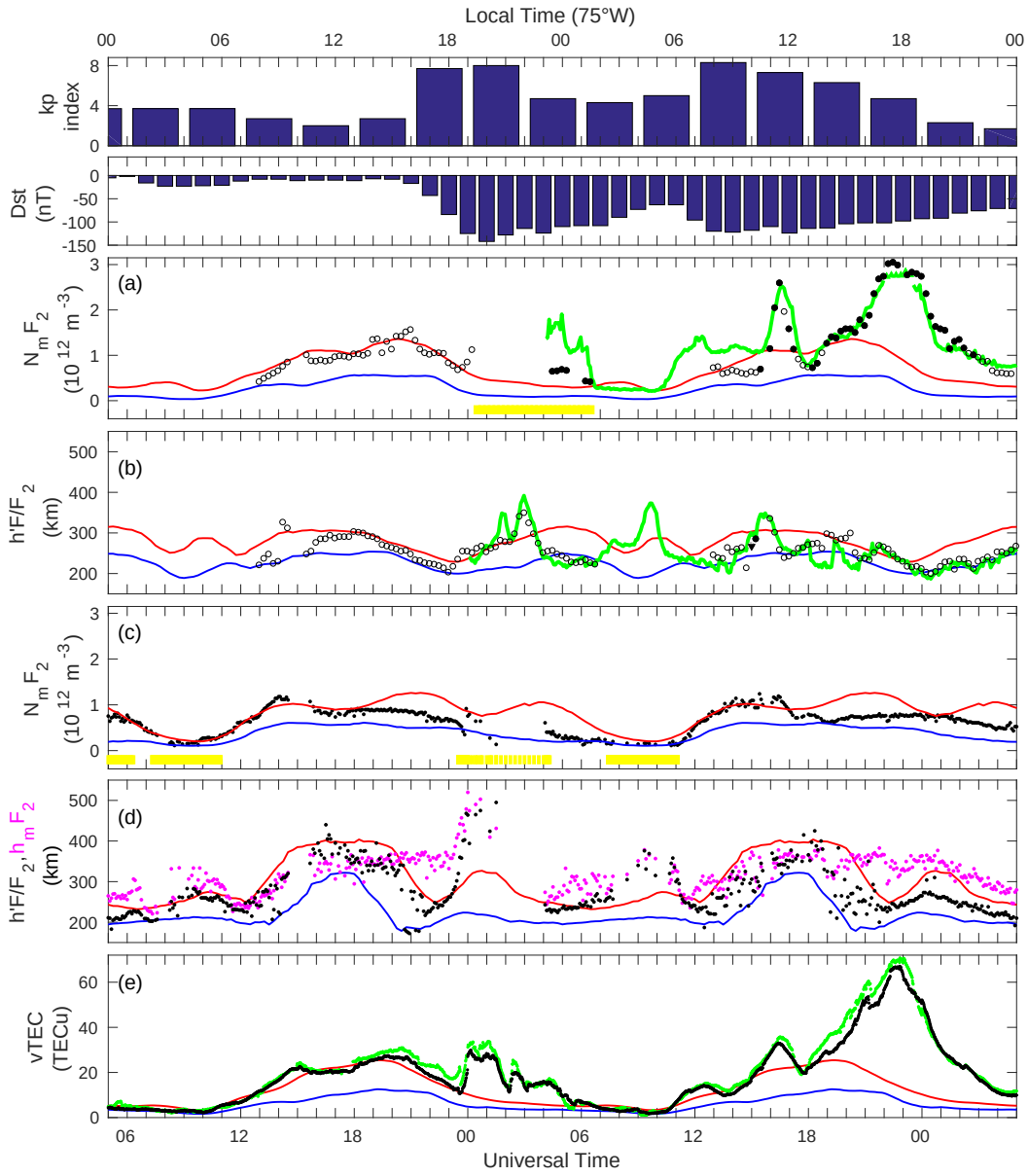


Fig. (4). Diurnal variations of global geomagnetic indices, ionospheric characteristics and vTEC for 7 (05:00-24:00 UT), 8 and 9 (00:00-05:00 UT) September 2017. (a) kp. (b) Dst. (c) NmF2 and (d) h'F/F2 at La Serena (LS, 29°52'S; 71°15'W) and Tucumán (TU, 26°50'; 65°14'W). (e) NmF2 and (f) h'F/F2 and hmF2 at Jicamarca (JI, 11°57'S; 78°52'W). (g) vTEC at LS and TU. Open circles, black filled circles and a black line are for LS; black filled circles are for those values scaled as "doubtful" according to international accepted rules [34]. Green lines are for TU. Black and magenta dots are for JI. Red lines are for smoothed median values plus interquartile range and blue lines are for the median minus interquartile range for 17 quiet days. The horizontal grey bars show spread-F intervals.

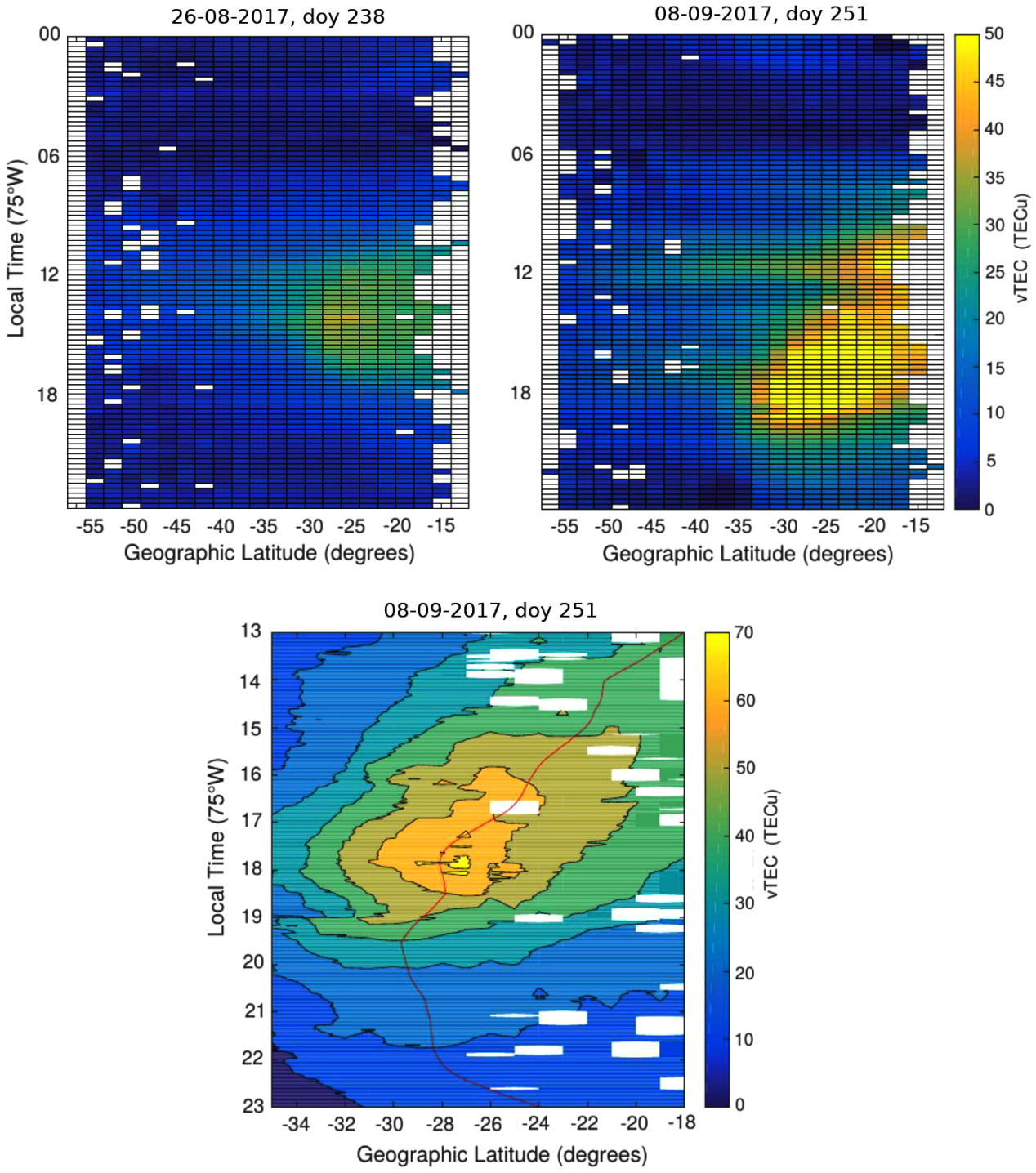


Fig. (5). Time latitude variation of vTEC for (top left) geomagnetically quiet day (26 August 2017) and (top right) storm day (8 September 2017), and (bottom) enlarged version of storm day (note different vTEC scale). (red line) latitude of maximum vTEC.

vTEC was also calculated as a latitude polynomial fit, for a given time, to vTEC values used for the smaller figure, also at one-minute resolution. Then, the latitude of maximum vTEC was calculated using the polynomial fit for each minute. The red line on the enlarged figure indicates the time evolution of the latitudinal maximum, after smoothing.

The development of the EIA for quiet times is clearly shown in Fig. (**5**). The latitude of maximum vTEC is at about 26°S and takes place at around 19:00 UT (14:00 LT). On the storm day, two separate events are evident. The first event is a short increase of vTEC (~ 2 h), has a large latitudinal extent (~ 30°), peaking almost simultaneously at all latitudes between 16:00-17:00 UT (11:00 and 12:00 LT), though the latitude

maximum seems to lay equatorward of the available vTEC values. It is recalled that this event is clearly seen in Fig. (**4**) and is identified as the third deviation. It is not clear whether the event can be associated with the development of the EIA. Some suggestions will be offered in the Discussion.

The second and much larger and longer event is then observed. The latitudinal maximum is clearly identified as moving steadily poleward of 15°S (the fourth deviation identified in Fig. (**4**). The enlargement of the 8 September 2017 variation shows that this latitudinal maximum southernmost location is found between 30 and 31°S at about 00:30 UT (19:30 LT). It is over TU at about 22:20 UT (17:20 LT) and over LS around 23:40 UT (18:40 LT). Moreover, maximum values of vTEC are attained within the 22:15-23:20 UT (17:15 -18:20 LT) time interval between 27 and 28°S. These two stages of the development match very well with the observations of the third and fourth deviations of NmF2 at LS and TU and of vTEC at TU, as described before (Section 3.2.1, Fig. (**4**), although the timing may show some differences. These differences arise from uncertainties on the NmF2 timing at LS and TU (see section 3.2.1) and the smoothing procedure used to determine the latitudinal maximum.

4. DISCUSSION

Some 24 hours before the onset of the geomagnetic storm, sudden changes in several interplanetary characteristics are observed at the L1 point by the ACE satellite [26]. The L1 point is a place in the Earth-Sun direction, where Sun's gravity is equal to Earth's gravity. The OMNIWeb data set (https://omniweb.gsfc.nasa.gov) shows that changes in solar wind velocity and pressure exhibit clear sudden increases at 23:50 UT (18:50 LT) of 6 September 2017. Unfortunately, there are no ionosonde observations available at LS for the following hours. However, available TEC values confirm that no changes are observed. Furthermore, ionograms at JI also show no significant changes. Thus, no further discussion was considered necessary.

It is recalled that while presenting the diurnal variations of various ionospheric characteristics during the 7 to 9 September 2017, four deviations from reference values were considered. Here a few suggestions are made to explain these deviations. In Fig. (**6**) are shown again the h'F/F2 diurnal variations of 7 and 9 September 2017, together with the associated changes of the Interplanetary Electric Fields (IEF), solar wind speed, magnetic pressure and the magnetic field Bz component given by the OMNIWeb data set and the incoherent scatter radar vertical drift (E×B drift) observations (ISR) at JI (http://jro-db. igp.gob.pe/madrigal). A quiet time reference E×B drift is also given [31].

The large increases of h'F/F2 and hmF2 observed at JI on 7 September 2017 are associated with the sudden changes of all interplanetary parameters during the 23:00-24:00 UT (18:00-19:00 LT) interval indicating the storm onset. These changes are followed within an hour by the ISR drift observed at JI. It seems that the penetration IEF increases the E×B drift which in turn lifts the F-region. The lift takes the concentration of the electrons from the F layer across the geomagnetic field lines at equatorial latitudes (fountain effect) and the subsequent downward diffusion along the field lines leading to increases of TEC at the crests of the EIA, and thus observed at LS and TU.

The second increase of h'F/F2 takes place in the morning of 8 September 2017 (07:00-11:00 UT; 02:00-06:00 LT) at TU and JI (no ionograms available at LS). This feature is associated with the increases of the ISR drift Fig. (**6f**) observed at JI between 07:00 and 11:00 UT (02:00 and 06:00 LT), including two small peaks. This night-time upward drift corresponds to negative IEF direction (Fig. (**6e**). A sudden switch in IEF polarity (12:00 UT = 07:00 LT), which coincides with other sudden changes of interplanetary characteristics during the Magnetic Ejecta phase of the ICME [26] does not seem to have any effect on ionospheric characteristics observed at all three locations (JI, TU and LS). This lack of significant effects may be expected because the events occur in the early morning, since the effects are attenuated after the evening change of the IEF sign and the night-time low concentration.

As already noted, the third clear increases of h'F/F2 at LS and TU peaking around 16:00 UT (11:00 LT) of 8 September 2017, are followed by large and short lived NmF2 peaks at LS and TU, and a very small increase at JI. This may be due to a quick increase of the fountain effect driving most of the ionization directly to the TU and LS latitudes without much effect on the equatorial ionosphere. It should be conceded, though, that no significant increases of E×B are observed at JI on the relevant time interval. Fig. (**6**) also shows that there is a little but sharp decrease of B_Z and a concurrent increase of P between 16:00 and 17:00 UT (11:00 and 12:00 LT). The simultaneous decrease of IEF obviously is related to the B_Z increase since it is derived from it, the other factor being V_{SW} which, for the corresponding interval, is almost constant. However, a similar situation, even more significant, is shown by these parameters earlier on, 15:00 to 16:00 UT interval (10:00 to 11:00 LT). A further search shows that it is only for the 16:00-17:00 UT (11:00-12:00 LT) interval that the proton temperature has a sharp peak (not shown in Fig. (**6**). Whether there is a relationship between proton temperature and NmF2 or vTEC at LS and TU needs to be confirmed. No relation is found on any of these intervals with AE index (an auroral index indicating intensity of electric currents along the auroral zone). Alternatively, it would be useful to explore the hypothesis of Batista *et al.* [32], which associates equatorial sharp changes (NmF2) with thermospheric wave-like winds effects. Thus, the physical mechanism for this third deviation is not clear.

The largest increases of NmF2 and TEC observed at LS and TU on 8 September 2017 at 23:00 UT (18:00 LT, Fig. (**4**), but not at JI, which are consistent with the systematic southward shift of the EIA, as determined from the time-latitude variation of TEC discussed in Section 3.2.2. There is also a small decrease of the ISR drift Fig. (**6f**) beginning at about 22:30 UT (17:30 LT) which may be interpreted as the effect of on equatorward wind (opposite to what is expected during daytime) since there is no consistent IEF signature. It is here suggested that an intensified EIA crest Fig. (**5**) is due to this increased equatorward thermospheric wind that uplift the F-region along the inclined geomagnetic lines [33].

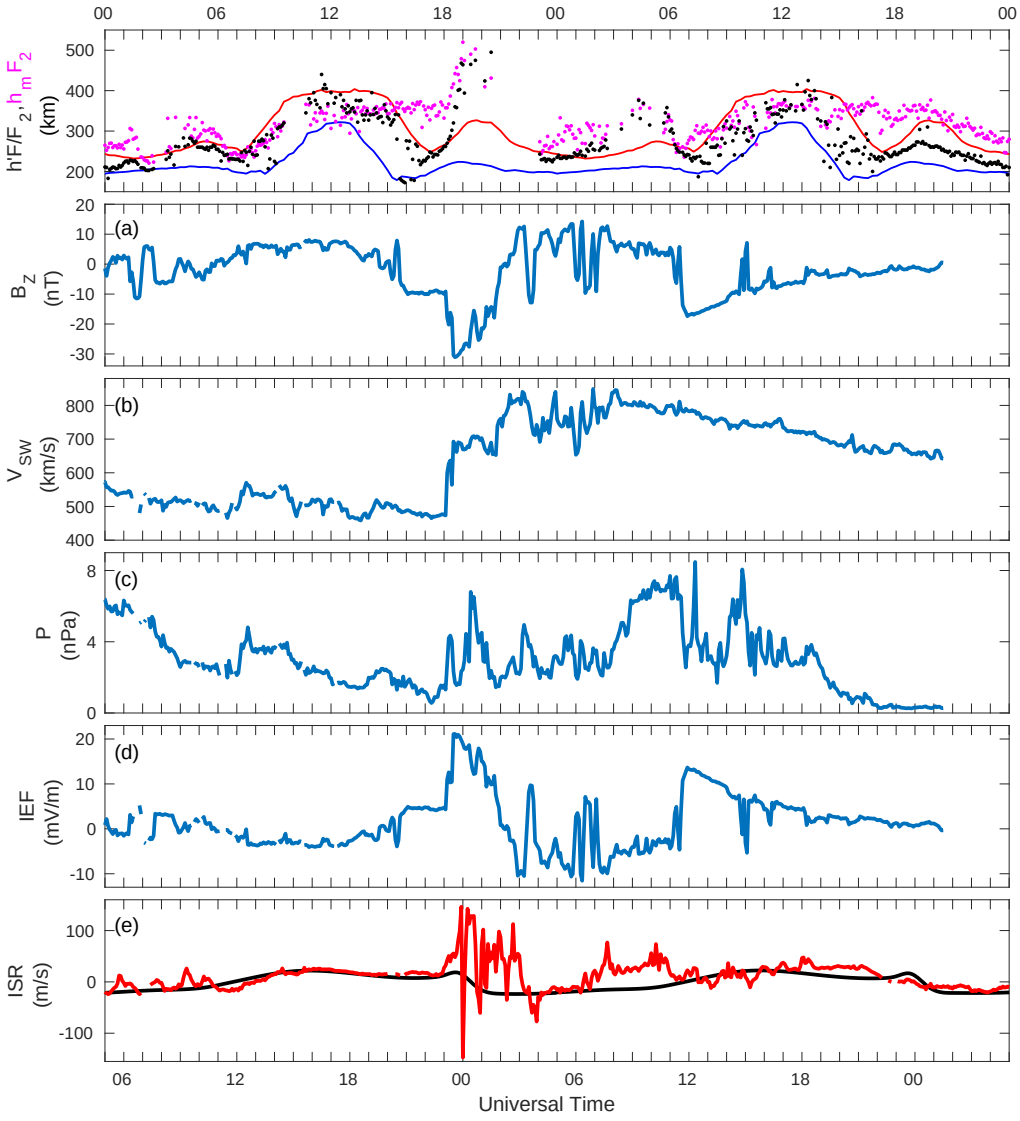


Fig. (6). Diurnal variations of ionospheric characteristics at Jicamarca (JI, 11°57'S; 78°52'W) and interplanetary L1 observations for 7 (05:00-24:00 UT), 8 and 9 (00:00-05:00 UT) September 2017. (a) h'F/F2 and hmF2 from Figure 4 at JI (black and magenta dots, respectively). (b) Magnetic Bz component. (c) Solar wind speed. (d) Solar wind pressure. (e) Interplanetary Electric Field. (f) (red) Incoherent scatter radar vertical drift and (black) quiet time reference drift at JI [31].

CONCLUSION

SIDs are observed at La Serena (29°52'S; 71°15'W) following most significant solar flares of 6 to 10 September 2017, in spite of some observations gaps. The SIDs are also simultaneously observed at Tucumán (26°50'; 65°14'W) and Jicamarca (11° 57'S; 78°52'W). Some indication on the evolution of the SIDs in two cases is also given, taking into account the various instrumental sensitivity differences. An estimation of the impairment of HF propagation paths is also suggested.

Geomagnetic storms ionospheric effects on NmF2, h'F/F2 and vTEC are reported for equatorial and low latitudes. Simultaneous increases of NmF2 and vTEC coincide with a large increase of equatorial h'F/F2 concurrent with the main phase of the storm during the evening (LT 75°W) of 7 September 2017. Increases of h'F/F2 at low latitudes are delayed by a couple of hours. By contrast, simultaneous increases of h'F/F2 at equatorial and low latitudes during the recovery phase are associated with concurrent decreases of NmF2 and vTEC. On a secondary recovery phase of the storm, increases of h'F/F2 at low latitudes are followed (by about an hour) by two very large increases of NmF2 and vTEC at low latitudes. One is around 8 September 2017 noon and the other in the evening. Increases are not observed at equatorial latitudes. The two events are clearly observed on the time-latitude variation of vTEC for the 70°W meridian. It is found that later effects are well described in terms of the evolution of the EIA over the same time interval. IEF and E×B variations are suggested to explain most of the observations, though alternatively, hypothesis related to thermospheric wave-like winds can be explored.

LIST OF ABBREVIATIONS

ACE	=	Advanced Composition Explorer
Bz	=	Magnetic Field z-component
CADI	=	Canadian Advanced Digital Ionosonde
CSN	=	Centro Sismológico Nacional
Dst	=	Disturbance storm time index
EIA	=	Equatorial Ionospheric Anomaly
GNSS	=	Global Navigation Satellite System
GPS	=	Global Positioning System
fmin	=	The lowest frequency at which an o-mode (ordinary) echo is observed on the ionogram
foE	=	E layer o-mode critical frequency
foF2	=	F2 layer o-mode critical frequency
ftEs	=	Top frequency of the Es trace (any mode)
h'E	=	E layer o-mode minimum virtual height
hmE	=	True height of E-layer
hmF2	=	True height of F2 peak
h'F/F2	=	F/F2 layer o-mode minimum virtual height
ICME	=	Interplanetary Coronal Mass Ejection
IEF	=	Interplanetary Electric Field
IGS	=	International GNSS Service
IPS	=	Ionospheric Prediction Service
ISR	=	Incoherent Scatter Radar
JI	=	Jicamarca station
LS	=	La Serena station
LT	=	Local Time
M3000F2	=	F2 layer M factor (ratio of the maximum usable frequency divided by the critical frequency)
NmF2	=	Maximum electronic density
P	=	Flow Pressure
RINEX	=	Receiver Independent Exchange Format
SIDs	=	Sudden Ionospheric Disturbances
sTEC	=	slant TEC
TEC	=	Total Electron Content
TU	=	Tucumán station
UT	=	Universal Time
Vsw	=	Solar Wind Velocity
vTEC	=	vertical TEC
ymD/E	=	semi-thickness of D/E-Layer
ymF2	=	semi-thickness of F2-Layer

ETHICS APPROVAL AND CONSENT TO PARTICIPATE

Not applicable.

HUMAN AND ANIMAL RIGHTS

No animals/ humans were used for the studies that are basis of this research.

CONSENT FOR PUBLICATION

Not applicable.

AVAILABILITY OF DATA AND MATERIALS

The Jicamarca ionograms and the scaled values of the ionospheric characteristics were obtained from the Digital Ionogram Data Base (DIDB) at http://ulcar.uml.edu/DIDBase/. Cesar Valladares kindly provided access to the Lowlatitude Ionospheric Sensor Network (LISN) from which the Tucumán ionograms were downloaded. LISN is a project led by the University of Texas at Dallas in collaboration with the Geophysical Institute of Perú, and other institutions that provide information for the benefit of the scientific community.

Access to ISR drifts is from Madrigal Database at Jicamarca Radio Observatory (http://jro-db.igp.gob.pe/ madrigal). Access to the GPS data was kindly offered by the Centro Sismológico Nacional, Universidad de Chile (www. sismologia.cl). Access to the GOES X-ray fluxes is from National Centers for Environmental Information (NCEI) of National Oceanic and Atmospheric Administration (NOAA) at https:// satdat.ngdc.noaa.gov. Access to L1 observations is from the OMNIWeb of Goddard Space Flight Center (GSFC) at https://omniweb.gsfc.nasa.gov.

FUNDING

Chilean ionospheric stations at La Serena and Chillán are operated under the auspices of the recently established Centro Interuniversitario de Física de la Alta Atmósfera (Interuniversity Centre of Upper Atmosphere Physics, CInFAA in Spanish) funded by Universidad de Concepción, Universidad Adventista de Chile and Universidad de La Serena.

CONFLICT OF INTEREST

The authors declare no conflict of interest, financial or otherwise.

ACKNOWLEDGEMENTS

MB acknowledges the support by CONICYT Anillo grant ACT1405 and CONICYT/FONDECYT POSTDOCTORADO 3180742. RL was supported by Proyecto Interno Universidad Adventista de Chile n° 79. LT and PV-J thanks the Dirección de Investigación y Desarrollo de la Universidad de La Serena, Project VIPDDI001 10201020936 PR18145. We are very grateful to the anonymous reviewers for their significant comments which lead to many text changes.

REFERENCES

[1] Prolss GW, von Zahn U. Esro 4 Gas Analyzer results 2. Direct measurements of changes in the neutral composition during an ionospheric storm. J Geophys Res 1974; 79(16): 2535-9. [http://dx.doi.org/10.1029/JA079i016p02535]

[2] Rishbeth H. F-region storms and thermospheric circulation. J Atmos Terr Phys 1975; 37: 1055-64. [http://dx.doi.org/10.1016/0021-9169(75)90013-6]

[3] Cesaroni C, Alfonsi L, Pezzopane M, Martinis C, Baumgardner J, Wroten J, *et al.* The first use of coordinated ionospheric radio and optical observations over Italy: Convergence of high-and low-latitude storm-induced effects. J Geophys Res Space Phys 2017; 122: 11794-806. [http://dx.doi.org/10.1002/2017JA024325]

[4] Malki K, Bounhir A, Benkhaldoun Z, *et al.* Ionospheric and thermospheric response to the 27–28 February 2014 geomagnetic storm over north Africa. Ann Geophys 2018; 36: 987-98. [http://dx.doi.org/10.5194/angeo-36-987-2018]

[5] Sobral J H A M A. Effects of intense storms and substorms on the equatorial ionosphere/thermosphere system in the American sector from ground-based and satellite data. J Geophys Res 1997; 102(A7): 14,305-13. [http://dx.doi.org/10.1029/97JA00576]

[6] Abdu MA, de Souza JR, Sobral JHA, Batista IS. Magnetic storm associated disturbance dynamo effects in the low and equatorial latitude ionosphere.Recurrent magnetic storms: Corotating solar wind streams. Washington, DC: American Geophysical Union 2006. [http://dx.doi.org/10.1029/167GM22]

[7] Batista IS, Abdu MA, Souza JR, *et al.* Unusual early morning development of the equatorial anomaly in the Brazilian sector during the Halloween magnetic storm. J Geophys Res 2006; 111A05307 [http://dx.doi.org/10.1029/2005JA011428]

[8] Nogueira PAB, Abdu MA, Batista IS, de Siqueira PM. Equatorial ionization anomaly and thermospheric meridional winds during two major storms over Brazilian low latitudes. J Atmos Sol Terr Phys 2011; 3: 1535-43. [http://dx.doi.org/10.1016/j.jastp.2011.02.008]

[9] Santos AM, Abdu MA, Souza JR, Sobral JHA, Batista IS. Disturbance zonal and vertical plasma drifts in the Peruvian sector during solar minimum phases. J Geophys Res Space Phys 2016; 121: 2503-21. [http://dx.doi.org/10.1002/2015JA022146]

[10] Rodger AS, Smith R. Antarctic studies of the coupled ionosphere-magnetosphere system. Philos Trans R Soc Lond 1989; 328: 271-87. [http://dx.doi.org/10.1098/rsta.1989.0036]

[11] Fuller-Rowell TJ, Rees D, Quegan S, *et al.* A coupled thermosphere-ionosphere model (CTIM)STEP Handbook of Ionospheric Models. Logan, Utah: Utah State University 1996; pp. 217-38.

[12] Rishbeth H, Müller-Wodgar ICF. Vertical circulation and thermospheric composition: a modelling study. Ann Geophys 1999; 17: 794-805. [http://dx.doi.org/10.1007/s00585-999-0794-x]

[13] Rishbeth H, Müller-Wodgar ICF, Zou L, *et al.* Annual and semiannual variations in the ionospheric F2-layer: II. Physical discussion. Ann Geophys 2000; 18: 945-56. a [http://dx.doi.org/10.1007/s00585-000-0945-6]

[14] Rishbeth H, Sedgemore-Schulthess KJF, Ulich T. Semiannual and annual variations in the height of the ionospheric F2-peak. Ann Geophys 2000; 18: 285-99. b [http://dx.doi.org/10.1007/s00585-000-0285-6]

[15] Zou L, Rishbeth H, Müller-Wodarg ICF, *et al.* Annual and semiannual variations in the ionospheric F2-layer: I. Modelling. Ann Geophys 2000; 18: 927-44. [http://dx.doi.org/10.1007/s00585-000-0927-8]

[16] Blagoveshchensky DV, Maltseva OA, Maria A, Sergeeva MA. Impact of magnetic storms on the global TEC distribution. Ann. Geophys. Discuss 2018.

[17] Buresova D, Lastovicka J. Differences in midlatitude ionospheric response to magnetic disturbances at Northern and Southern Hemispheres and anomalous response during the last extreme solar minimum.Ionospheric Space Weather: Longitude and Hemispheric Dependences and Lower Atmosphere Forcing AGU Geophys Monograph. J. Wiley&Sons 2017; pp. 41-58.

[18] Lin CH, Hsiao CC, Liu JY, Liu CH. Longitudinal structure of the equatorial ionosphere: Time evolution of the four-peaked EIA structure. J Geophys Res 2007; 112A12305 [http://dx.doi.org/10.1029/2007JA012455]

[19] Reddy CD, Shrivastava MN, Seemala G, González G, Baez JC. Ionospheric Plasma Response to Mw 8.3 Chile Illapel Earthquake on September 16, 2015.The Chile-2015 (Illapel). Cham: Earthquake and Tsunami. Pageoph Topical Volumes. Birkhäuser 2016.

[20] Ovalle EM, Villalobos CU, Agüero LA, Leiva RE, Foppiano AJ. A new ionospheric station for Chile Bulletin No 74, Ionospheric Network Advisory Group, Union Radio Scientific Internationale 2017.

[21] Galkin I. URSI Working Group G.-1, Ionosonde Network Advisory Group Business Meeting XXXIInd URSI General Assembly and Scientific Symposium. Montreal, Canada. 2017.August 23, 2017;

[22] Titheridge JE. Updated software for ionogram recording and analysis INAG Bulletin No 62, Commission G, Working Group G 1, International Union of Radio Science 1998.

[23] Ratcliffe JA. Magneto-Ionic Theory & its Applications to the Ionosphere. Cambridge University Press 1959.

[24] Seemala GK, Valladares CE. Statistics of total electron content depletions observed over the South American continent for the year 2008. Radio Sci 2011; 46RS5019 [http://dx.doi.org/10.1029/2011RS004722]

[25] Redmon R J, Seaton D B, Steenburgh R, He J, Rodriguez J V. Space Weather Events of 4–10 September 2017 September 2017's Geoeffective Space Weather and Impacts to Caribbean Radio Communications during Hurricane Response Space Weather Journal 2018.

[26] Schwadron NA, Rahmanifard F, Wilson J, Jordan AP, Spence HE, Joyce CJ, *et al.* Update on the worsening particle radiation environment observed by CRaTER and implications for future human deep space exploration. Space Weather 2018; 16: 289-303. [http://dx.doi.org/10.1002/2017SW001803]

[27] Liu JY, Lin CH, Chen YI, *et al.* Solar flare signatures of the ionospheric GPS total electron content. J Geophys Res 2006; 111A05308 [http://dx.doi.org/10.1029/2005JA011306]

[28] Yasyukevich Y, Astafyeva E, Padokhin A, Ivanova V, Syrovatskii S, Podlesnyi A. The 6 September 2017 X-class solar flares and their impacts on the ionosphere, GNSS, and HF radio wave propagation. Space Weather 2018; 16(8): 1013-27. [http://dx.doi.org/10.1029/2018SW001932] [PMID: 31031571]

[29] Appleton EV. Two Anomalies in the Ionosphere. Nature 1946; 157: 691. [http://dx.doi.org/10.1038/157691a0]

[30] Ratcliffe JA. Sun, Earth, and Radio: An Introduction to the Ionosphere and Magnetosphere World University Library Series. London, UK: Weidenfeld and Nicolson Publishing 1970.

[31] Scherliess L, Fejer BG. Radar and satellite global equatorial F region vertical drift model. J Geophys Res 1999; 104(A4): 6829-42. [http://dx.doi.org/10.1029/1999JA900025]

[32] Batista IS, Abdu MA, Nogueira PAB, *et al.* Early morning enhancement in ionospheric electron density during intense magnetic storms. Adv Space Res 2012; 49(11): 1544-52. [http://dx.doi.org/10.1016/j.asr.2012.01.006]

[33] Balan N, Shiokawa K, Otsuka Y, Watanabe S, Bailey GJ. Super plasma fountain and equatorial ionization anomaly during penetration electric field. J Geophys Res 2009; 114A03310 [http://dx.doi.org/10.1029/2008JA013768]

[34] URSI Handbook of Ionogram Interpretation and Reduction In: Report UAG-23A, International Union of Radio Science. second edition.

© 2019 Bravo *et al.*

This is an open access article distributed under the terms of the Creative Commons Attribution 4.0 International Public License (CC-BY 4.0), a copy of which is available at: https://creativecommons.org/licenses/by/4.0/legalcode. This license permits unrestricted use, distribution, and reproduction in any medium, provided the original author and source are credited.

View publication stats